Biosensors and Bioelectronics 25 (2009) 55–60

Contents lists available at ScienceDirect

Biosensors and Bioelectronics

journal homepage: www.elsevier.com/locate/bios

Real-time monitoring of odorant-induced cellular reactions using surface plasmon resonance

Sang Hun Lee, Hwi Jin Ko, Tai Hyun Park*

School of Chemical and Biological Engineering, Institute of Bioengineering, Seoul National University, Gwanak-Gu, Sillim-Dong, San 56-1, Seoul, 151-744, Republic of Korea

ARTICLE INFO

Article history:
Received 14 April 2009
Received in revised form 1 June 2009
Accepted 2 June 2009
Available online 10 June 2009

Keywords:
Olfactory receptor I7
Human embryonic kidney (HEK)-293 cell
Olfactory biosensor
Surface plasmon resonance

ABSTRACT

Surface plasmon resonance (SPR) is a powerful technique for measuring molecular interaction in real-time. SPR can be used to detect molecule to cell interactions as well as molecule to molecule interactions. In this study, the SPR-based biosensing technique was applied to real-time monitoring of odorant-induced cellular reactions. An olfactory receptor, OR I7, was fused with a rho-tag import sequence at the N-terminus of OR I7, and expressed on the surface of human embryonic kidney (HEK)-293 cells. These cells were then immobilized on a SPR sensor chip. The intensity of the SPR response was linearly dependent on the amount of injected odorant. Among all the aldehyde containing odorants tested, the SPR response was specifically high for octanal, which is the known cognate odorant for the OR I7. This SPR response is believed to have resulted from intracellular signaling triggered by the binding of odorant molecules to the olfactory receptors expressed on the cell surface. This SPR system combined with olfactory receptor-expressed cells provides a new olfactory biosensor system for selective and quantitative detection of volatile compounds.

1. Introduction

The mammalian olfactory system can detect and discriminate a great number of structurally diverse odorant molecules (Buck and Axel, 1991). The first event in the detection of these different odorants is the specific binding between the odorant molecules and olfactory receptors (ORs). This binding changes the conformation of OR and triggers the activation of an intracellular signaling cascade via a specific G-protein. The G-protein activates adenylyl cyclase, leading to an increase in intracellular cyclic adenosine monophosphate (cAMP) levels. The increased cAMP activates an olfactory-specific cyclic nucleotide gated (CNG) channel. The opened CNG channel leads to an influx of intracellular Ca^{2+} and Na^{+} and the subsequent opening of the Ca^{2+}-activated Cl^{-} channel (Firestein, 2001; Krautwurst et al., 1998; Malnic et al., 1999). The discovery of the multigene family encoding ORs opened the way for both fundamental and biotechnological investigations. Expression and characterization of olfactory receptors have been carried out in various different heterologous systems, and progress in understanding the olfactory system has resulted in the development of artificial odor-sensing systems (Ko and Park, 2005; Matarazzo et al., 2005; Sung et al., 2006; Vidic et al., 2006; Lee et al., 2009). A large portion of this progress is based on the olfactory receptors themselves.

The function of olfactory receptors expressed in heterologous cells, such as HEK-293 cell, Sf9 cell, HeLa cell, Yeast, and *E. coli* have been investigated, and biosensors that utilize these olfactory receptors have been developed. Olfactory receptors have been coupled with electronic devices in order to design a new family of bioelectronic noses. Biosensors combine the inherent specificity of the recognition elements with the high sensitivity of various physical transducers, enabling selective and sensitive detection of the analytes of interest. In recent years, many techniques such as quartz-crystal microbalance (QCM), electrochemical impedance spectrometry (EIS), surface plasma resonance (SPR), and light-addressable potentiometric (LAPS) sensor have been used as the physical transducer component of biolectronic noses (Hou et al., 2007; Lee et al., 2006; Marrakchi et al., 2007; Sung et al., 2006; Vidic et al., 2007; Wu et al., 2009). These biosensors were developed based on the specific interaction between olfactory receptors and odorant molecules, and have many potential applications in a wide range of different fields, i.e. medicine, environment, food, cosmetic or fragrance industries, etc.

SPR is a well-known and powerful technique that can measure molecular interactions on the surface of a sensor chip in real-time without any labeling. SPR is highly sensitive to small changes in the refractive index occurring at the surface of a thin noble metal film. Furthermore, among the various optical sensing methodologies, the SPR-based sensor has been widely regarded as one of the best tools for detecting biomolecules, enzymatic reactions, structural changes and detection of pathogen (Helali et al., 2008; Joung

* Corresponding author. Tel.: +82 2 880 8020; fax: +82 2 875 9348.
E-mail address: thpark@snu.ac.kr (T.H. Park).

0956-5663/$ – see front matter © 2009 Elsevier B.V. All rights reserved.
doi:10.1016/j.bios.2009.06.007

et al., 2007; Mazumdar et al., 2007). Recently, several studies have attempted to use SPR to investigate cellular reactions in whole cell. From these studies, it was reported that SPR sensors can detect changes in resonance angle, which results from cell–ligand interactions, positioning and adhesion of immobilized cells on sensor chip surface (Hide et al., 2002; Yanase et al., 2007). In this study, we applied the SPR-based biosensing technique to detect binding between olfactory receptors and odorant molecules. Genetically modified HEK-293 cells expressing OR were loaded on the SPR chip, and their SPR response to odorant stimulation was measured.

2. Materials and methods

2.1. Reagents

The running buffer (Ca^{2+} standard buffer) for SPR analysis consisted of the following: 140 mM NaCl, 5.4 mM KCl, 1 mM $MgCl_2$, 10 mM HEPES (pH 7.4), 5 mM glucose and 2 mM $CaCl_2$. The Ca^{2+}-free buffer contained 2 mM EGTA instead of 2 mM $CaCl_2$, and the other components were the same as the Ca^{2+} standard buffer. The phosphate-buffered saline (PBS, pH 7.4) consisted of 137 mM NaCl, 2.7 mM KCl, 10 mM Na_2HPO_4 and 1.8 mM KH_2PO_4. These chemicals, and dimethyl sulfoxide (DMSO), 99% ethanol and poly-D-lysine were purchased from Sigma–Aldrich (USA). Polyclonal anti-mouse Cy2 antibody and lipofectamine were purchased from Amersham-Pharmacia Biotech (UK). *Taq* polymerase, restriction enzymes and DNase were purchased from Takara (Japan). Dulbecco's modified Eagle's medium (DMEM), fetal bovine serum (FBS), penicillin and streptomycin were all purchased from GIBCO BRL (USA).

2.2. Cloning of olfactory receptor gene

A rho-tag import sequence was fused at the N-terminus of the rat olfactory receptor protein (OR I7) to target the receptor protein onto the cell membrane surface. The *rho-I7* fusion gene was cloned into an expression vector pcDNA3 (Invitrogen). The OR *I7* gene was amplified by PCR with pVL17 using the following primers: I7-N (EcoRI); 5′-GAATTCATGGAGCGAAGGAAC-3′, I7-C (XhoI); 5′-TCTCTCGAGGACCTAACCAATT-3′. PCR was performed with a mixture of *Taq* polymerase, 1.5 mM $MgCl_2$, 0.2 mM dNTPs, 0.5 mM of each primer, and 100 ng plasmids using the following temperature cycle: 35 cycles of 94 °C for 5 min, 55 °C for 30 s, and 72 °C for 1 min. The PCR product was digested with EcoRI and XhoI restriction enzymes and eluted through gel electrophoresis. The products were then ligated to pcDNA3-rho, which was digested by the same enzymes. Correct clone was confirmed by DNA sequencing.

2.3. Culture and transfection of HEK-293 cells

HEK-293 cells were grown in DMEM supplemented with 10% FBS, 100 U/ml penicillin, and 100 μg/ml streptomycin. Transfection with pcDNA3-rho-OR I7 was performed with lipofectamine. The HEK-293 cell lines stably expressing the OR I7 were selected by treatment with G418 (500 μg/ml) for a 2–3-week period. The cell surface expression of the OR I7 was identified by immnofluorescence signal and RT-PCR, which was performed as described in our previous study (Ko and Park, 2006). Cells stably expressing OR I7 were harvested by pipetting without trypsinization and directly cultured on SPR sensor chips (2×10^5 cells). Cells were not trypsinized to minimize the negative effect such as the inactivation of cell surface receptor.

2.4. Preparation of odorant solutions

Stock solutions of odorants (1 M) were prepared in DMSO and further dilutions (from 10^{-1} M to 10^{-4} M) were obtained by 1:10 dilutions in Ca^{2+} standard solution. Each diluted odorant solution was freshly prepared from a 1 M odorant stock on the day of the experiment. The Ca^{2+} standard solution, which was used as the running buffer, contained the same percentage of DMSO as the odorant solutions to compensate for possible bulk effects of DMSO in odorant detection. The concentration of DMSO was adjusted to 1% in the buffer solutions and odorant solutions. Octanal, which is specific to the OR I7 receptor, was used as the odorant. To study the effect of solvent DMSO on odorant detection, a DMSO solution was prepared in the exact same way as the octanal solution, where octanal was replaced by the same volume of ultrapure water.

2.5. Analysis using SPR

Since SPR reflects the events in the field of evanescence, the cells needed to be fixed on the sensor chip. The SPR chip was sterilized by autoclave, and gold surface of the SPR chip was treated with 0.1 mg/ml poly-D-lysine for stable attachment of cells. After incubation with 0.1 mg/ml poly-D-lysine for approximately 2 h at 4 °C, the gold surface was washed five times with deionized water and then immersed in 70% ethanol. The chip was then sterilized by ultraviolet irradiation for 1 day, and rinsed five times with PBS before use. Cells were seeded on the sterilized gold chip and incubated in DMEM supplemented with 10% FBS. HEK-293 cells were cultured to allow for strong adherence to the gold surface.

For the SPR system, SPRi (K-MAC, Korea) and sensor chips (18 mm × 18 mm) with bare gold surface were used. A slide glass and prism (n_D = 1.515, BK 7) were loaded onto a computer-controlled rotating stage. Optical contact between the prism and slide glass was achieved using a refractive index matching fluid (n_D = 1.515–1.517, Merck). The sensor chip, with a 50 nm thick gold film, was positioned in the flow cell unit of the SPR apparatus. The cells were perfused with running buffer at a flow rate of 50 μl/min and the odorant was injected from the side of the inlet. A p-polarized laser at 670 nm was used as the probe beam. Laser light was directed to the back of the sensor chip and the SPR system monitored the shift in reflectance. Reflected intensity was measured with a photodiode detector. The temperature was kept constant at 25.0 ± 0.1 °C during the measurement.

3. Results and discussion

3.1. Cell-based measurement of odorant using SPR

A schematic diagram showing the principles behind cell-based measurements of odorant molecules using SPR is shown in Fig. 1. The detectable evanescent field on the SPR gold surface is about 200 nm (Rossi et al., 2003), while the thickness of the cell is several micro-meters. Since the olfactory receptors are expressed on the surface of cells, the distance between the olfactory receptor and the gold surface is much longer than the detectable range. Therefore, the actual binding event between the olfactory receptor on the cell surface and the odorant molecule cannot be detected by SPR. However, this binding event still triggers intracellular signal transduction, which causes changes in intracellular components. Ca^{2+} ion influx through CNG channel or an endogenous channel is the main influx into cells than other ions (Firestein, 2001). These intracellular changes may generate a change in the SPR signal. The QCM signal shown in our previous work was the result of a simple binding interaction between the olfactory receptor and odorant (Sung et al., 2006). However, the SPR signals are believed to be the result of intracellular signaling induced by the binding of odorants to olfactory receptors. The OR I7 was chosen as the olfactory receptor in this study because its specific ligands are well documented (Zhao et al., 1998). Like all other GPCRs, OR

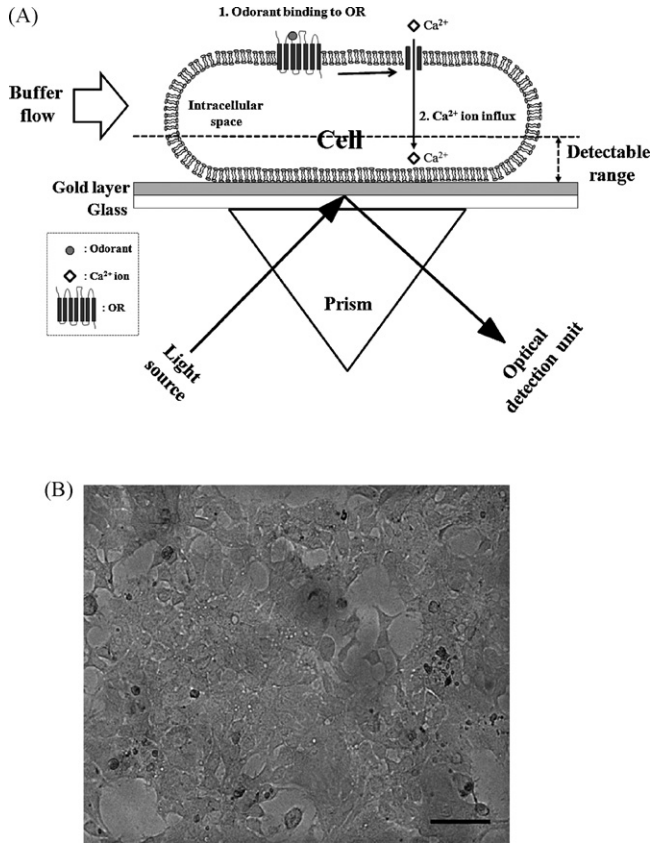

Fig. 1. Principle of olfactory biosensor for odorant detection using SPR. (A) Schematic representation of the sensor surface. B) Micrograph of cells cultured on the surface of SPR chip. The scale bar is 40 μm.

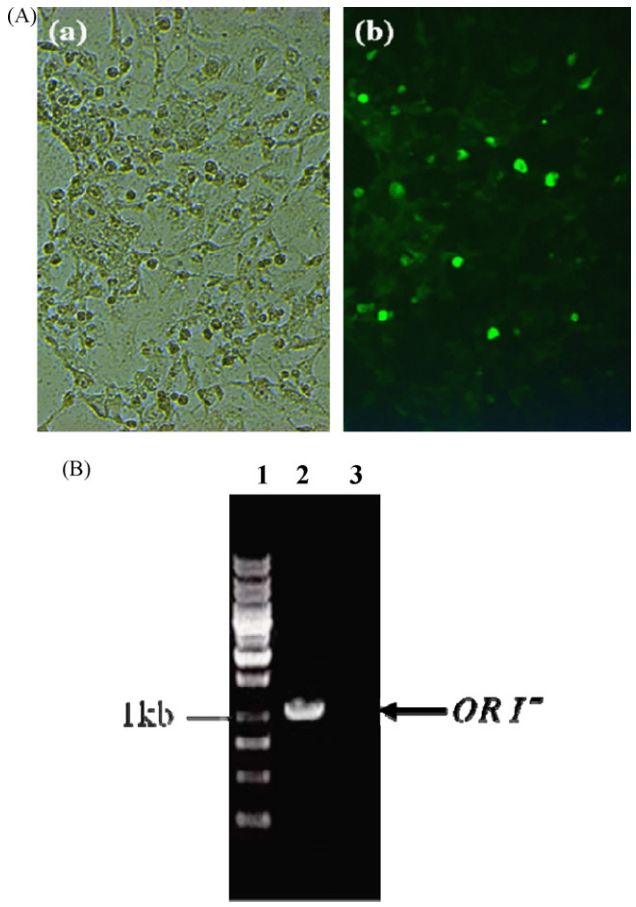

Fig. 2. Expression of olfactory receptor I7. (A) Immunocytochemistry. (a and b) represent optical and fluorescent images, respectively. The cells, which have surface expression of rho-I7 fusion proteins, were treated with a B6-30 primary antibody bound against a rho-tag import sequence. Then they subsequently treated with a Cy2-labeled secondary antibody (goat anti-mouse IgG). Surface expression of the rho-I7 fusion proteins was visualized by fluorescence, which was observed under a microscope with an excitation wavelength of 488 nm and an emission wavelength of 506 nm (Nikon, TE300, Japan). (B) RT-PCR of OR I7 gene. The 984 bp band corresponds to the mRNA of I7. Lane 1: size marker; lane 2: HEK-293 cells expressing OR I7; lane 3: wild type HEK-293 cell.

I7 contains seven transmembrane-spanning helices, which makes the receptor extremely hydrophobic, and therefore, it requires a lipidic environment to maintain its native conformation and functionality (Singer, 2000; Stenlund et al., 2003). In this study, the olfactory receptor I7 was expressed in HEK-293 cells and the whole cell was used as the sensing element. To express the I7 protein on the cell surface, a rho-tag import sequence was fused to the N-terminus of the receptor protein as described in our previous study (Ko and Park, 2006). HEK-293 cells were transfected with pcDNA3-rho-OR I7, and stable expression of I7 was confirmed by RT-PCR and an immunocytochemical method (Fig. 2(A) and (B)).

3.2. SPR responses of cells expressing OR I7

Odorant molecules are often hydrophobic and DMSO is usually used to dissolve the odorants in an aqueous solution. However, non-specific adsorption of DMSO on the SPR gold surface causes artifacts to appear in the SPR signal. In order to assess the magnitude of the undesirable effects of DMSO, control tests were performed. DMSO concentration in Ca^{2+} standard solutions was adjusted to 1%, 5%, and 10%. Each solution containing different DMSO concentrations was injected onto bare Au chip without cells. The SPR signal linearly increased with increasing DMSO concentration in the buffer solution (data not shown), and the reflectance increased by 1.5% when 1% DMSO was used. This effect may have resulted from a different reflective index between DMSO and the aqueous solution. Therefore, the DMSO concentration was fixed at 1% in every buffer and odorant solution used in subsequent experiments to minimize the artifacts caused by DMSO.

The SPR response of cells expressing OR I7 after odorant addition is shown in Fig. 3. HEK-293 cells expressing OR I7 were exposed to octanal in a Ca^{2+}-standard (Fig. 3(A)) and Ca^{2+}-free solution (Fig. 3(B)). After the binding of odorant and olfactory receptor, the triggered signal transduction ultimately leads to influx of Ca^{+} ions (Firestein, 2001; Krautwurst et al., 1998; Malnic et al., 1999). Consequently the influx of Ca^{+} ions into cells generated the SPR signal change. 10 mM octanal was continuously injected at a flow rate of 50 μl/min from 120 s to 240 s as shown in Fig. 3. The SPR signal change was observed only when the Ca^{2+} standard solution was used, and not when the Ca^{2+}-free solution was used.

Octanal was injected at 120 s, and the SPR signal began to increase at 180 s. The reflectance reached a maximum at 240 s when the octanal injection was stopped. When the odorant injection was stopped, the signal remained at the maximum level for approximately 60 s. The existence of this prolonged signal even after the odorant injection was stopped implies that the simple binding between the odorant and the OR protein was not solely responsible for generating this signal. After 60 s the signal began to decrease and took approximately 180 s to return to the basal level after the odorant injection was stopped.

In contrast, when cells expressing OR I7 were exposed to octanal in Ca^{2+}-free solution, no SPR signal was detected as shown in

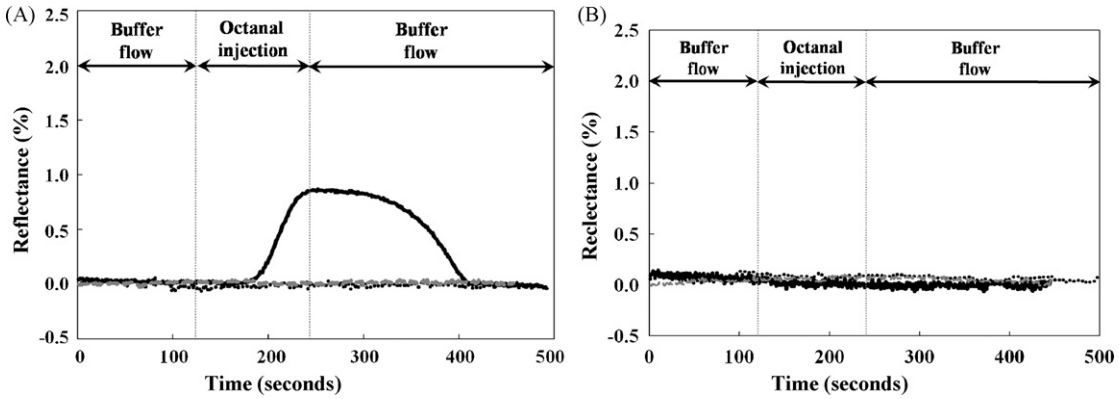

Fig. 3. SPR response to the injection of odorant in Ca^{2+} standard solution (A) and in Ca^{2+}-free solution (B). HEK-293 cells expressing the I7 were seeded on the sterilized SPR chip and incubated in DMEM supplemented with 10% FBS for strong adherence to the gold surface. The cells were perfused with running buffer at a flow rate of 50 μl/min and 10 mM octanal was continuously injected from the side of the inlet from 120 s to 240 s. Black solid line: 10 mM octanal; black dotted line: 0 mM octanal; gray dashed line: 10 mM octanal injection to wild type cells.

Fig. 3(B). These results indicate that the generated SPR signal is a reflection of the ensuing Ca^{2+} influx triggered by odorant binding to the olfactory receptor. The SPR signal change may be possibly caused by the transient change of cytoskeleton triggered by Ca^{2+} influx (Pfeiffer et al., 1985).

Our previous results obtained from the experiment using a channel blocker support that the binding of odorant with olfactory receptor induces the Ca^{+} influx through intrinsic transmembrane ion channels. When the HEK-293 cells expressing I7 were treated with $MgCl_2$, a channel blocker, the Ca^{+} influx was inhibited in a Ca^{2+} standard solution (Ko and Park, 2006). This result suggests that HEK-293 cells express the cationic channels through which Ca^{2+} ions are transported from the outside of the cell into the cytoplasm when the receptor is activated by odorant.

The injection of a control solution without octanal did not induce any signal change in both Ca^{2+}-containing and Ca^{2+}-free solutions (dotted line in Figs. 3(A) and (B)). In addition, no change in the SPR signal was detected in wild type HEK-293 cells, which was used as another control test, in both solutions (dashed line in Figs. 3(A) and (B)). These combined results suggest that Ca^{2+} ions are transported from outside of the cell into the cytoplasm through endogenous cationic channels in HEK-293 cells when the OR is activated by an odorant.

3.3. Dose-dependent SPR responses

In order to investigate the dose-dependent relationship between odorant and cellular response, various concentrations of octanal were applied to cells expressing OR on the SPR chip. Following immobilization of the cells expressing OR I7 to the chip, SPR signals were measured after injection of various concentrations of octanal in Ca^{2+} standard solution. As shown in Fig. 4(A), the SPR response increased with increasing octanal concentration. According to our previous results, intracellular Ca^{2+} concentration as well as cAMP level increased with octanal concentration (Ko and Park, 2006). This indicates that higher concentrations of odorant induced a greater change in the intracellular concentration of molecules involved in the signal transduction, which consequently resulted in the higher intensity of the SPR signal.

The upper and lower limit of the measurement was 10^{-1} and 10^{-4} M, respectively. The SPR response was not reproducible at higher concentrations (1 M). This is considered to be due to the toxicity of high concentration of odorant to the cells. The SPR response was also not detected at concentrations lower than 10^{-4} M. The correlation between maximum reflectance and odorant concentration is shown in Fig. 4(B). Data were obtained from at least 3 independent experiments. The dose-dependent response profiles have

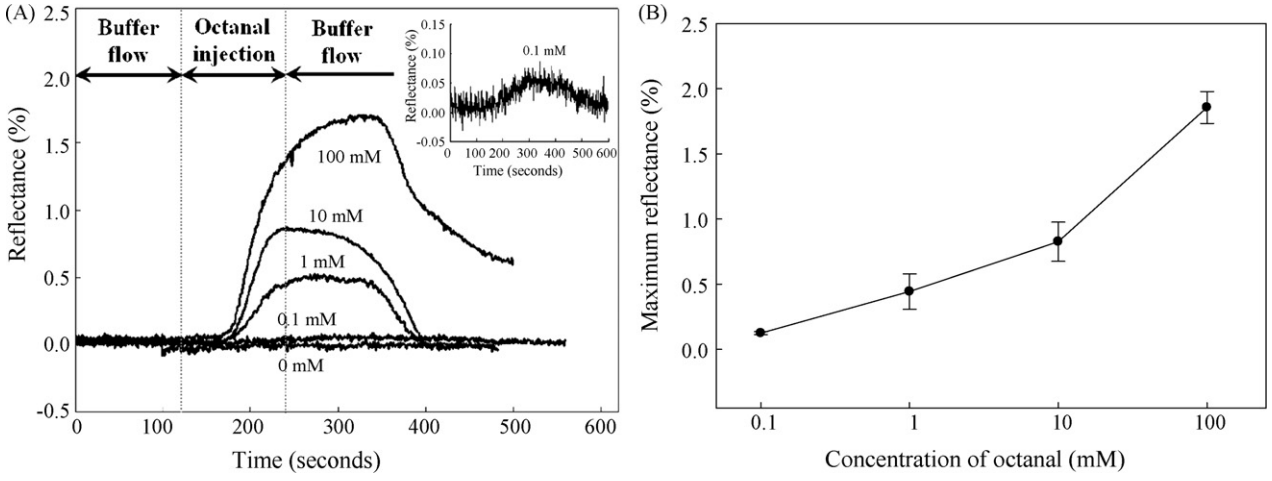

Fig. 4. Dose-dependent response of SPR after odorant injection. The SPR signal measurement procedures were same as in Fig. 3. (A) Dose-dependent curve of the SPR response to different concentrations of octanal. Inset curve represents the SPR response after injection of 100 μM octanal. (B) Relationship between maximum reflectance and odorant concentration. The maximum reflectance increases with the logarithmic value of octanal concentration. Data were obtained from at least three independent experiments (mean ± SD).

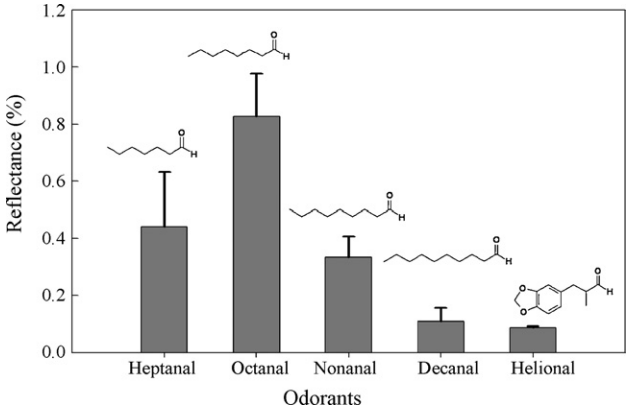

Fig. 5. Odorant specificity of HEK-293 cells stably expressing olfactory receptor I7. The *Y*-axis represents the reflectance produced by the change of intracellular Ca^{2+} ions in HEK-293 cells expressing olfactory receptor I7. The SPR response to octanal is the highest among the aldehyde odorants. Cells were stimulated with 10^{-2} M odorant. The error bars denote ±SD ($n = 3$).

been reported in the range of 10^{-7}–10^{-5} M for cell-based intracellular Ca^{2+} fluorescence assay (Araneda et al., 2004), 10^{-6}–10^{-1} M for cell-based electroolfactogram (Zhao et al., 1998), and 10^{-6}–10^{-5} M for olfactory cell-based light-addressable potentiometric sensor (Liu et al., 2006). Typical adsorption curve with a broad linear range (10^{-11}–10^{-2} M) was obtained from olfactory receptor-based QCM (Ko and Park, 2005), and 10^{-9}–10^{-5} M was the range for nanosomes containing olfactory receptor-based SPR (Vidic et al., 2006).

Compared with the methods described above, the sensitivity of the olfactory receptor combined with SPR turned out to be relatively lower. Incorporation of high influx ion channels into the cell membrane would increase the sensitivity. Physical formation of a specific plasmonic structure including deposition of gold nanoparticles, nanograting, and nanopatterning would also contribute to the higher sensitivity (Zhang et al., 2008).

3.4. Selective detection of odorants

The SPR response to various odorants is shown in Fig. 5. Cells expressing OR I7 were exposed to various odorants that contained an aldehyde group, such as heptanal (C7), octanal (C8), nonanal (C9) and decanal (C10). Cells were stimulated with an odorant concentration of 10^{-2} M. The SPR response was much higher for octanal, which is the known cognate odorant for the OR I7. Helional, which is the specific odorant ligand of a human olfactory receptor (hOR17–40) (Wetzel et al., 1999) and has a completely different chemical structure than octanal, was use as an odorant control. When helional was injected onto the cells, only a negligible SPR signal was detected in comparison to octanal. This result suggests that the SPR assay, which was based on immobilized HEK-293 cells expressing OR, was capable of recognizing and detecting only the specific target odorant.

4. Conclusions

In this study, we demonstrated that it was possible to directly measure odorant-induced cellular responses using SPR. Real-time monitoring of odorant-induced cellular reactions was demonstrated using a SPR system that was combined with olfactory receptor-expressed cells. The odorant-induced response was due to cellular signaling that was triggered by odorant binding to the olfactory receptor expressed on the cell surface. The key features of this system was the expression of olfactory receptors on the cell surface, the intracellular signal transduction triggered by the specific binding of odorants to the olfactory receptors, and the SPR response generated by the intracellular change. The SPR response to the odorant molecules was quantitative and selective. It was linearly dependent on the odorant concentration and specific to the odorant molecule that is the known cognate odorant for the specific olfactory receptor used in these experiments. The response signal was much lower when other odorant molecules with very similar chemical structures and properties were used. Multiplexing of various olfactory receptors on an array-type SPR chip element would prove to be more useful in the development of a biooptical nose.

Acknowledgements

This work was supported by the Korea Science and Engineering Foundation (KOSEF) grant funded by the Korea government (MEST) (No. 2009-0080242). The authors wish to acknowledge Dr. Randall R. Reed (Department of Neurosceince, Johns Hopkins University, School of Medicine, Baltimore, Maryland, U.S.A.) for the rho-tag gene; Akihito Yasuoka (Bio-oriented Technology Reseach Advancement Institution, Saitama, Japan) for the pVL-I7 and Paul A. Gargrave (J. Hillis Miller Health Center, Department of Ophthalmology, University of Florida College of Medicine, Gainesville, Florida, U.S.A.) for the B6-30 cell line.

References

Araneda, R.C., Peterlin, Z., Zhang, X., Chesler, A., Firestein, S., 2004. J. Physiol. 555, 743–756.
Buck, L., Axel, R., 1991. Cell 65, 175–187.
Firestein, S., 2001. Nature 413, 211–218.
Helali, S., Fredj, H.B., Cherif, K., Abdelghani, A., Martelet, C., Jaffrezic-Renault, N., 2008. Mater. Sci. Eng. C 28, 588–593.
Hide, M., Tsutsui, T., Sato, H., Nishimura, T., Morimoto, K., Yamamoto, S., Yoshizato, K., 2002. Anal. Biochem. 302, 28–37.
Hou, Y., Jaffrezic-Renault, N., Martelet, C., Zhang, A., Minic-Vidic, J., Gorojankina, T., Persuy, M.-A., Pajot-Augy, E., Salesse, R., Akimov, V., Reggiani, L., Pennetta, C., Alfinito, E., Ruiz, O., Gomila, G., Samitier, J., Errachid, A., 2007. Biosens. Bioelectron. 22, 1550–1555.
Joung, H.-A., Shin, W.-B., Chung, D.-H., Ahn, J., Chung, B.H., Choi, H.-S., Ha, S.-D., Kim, K.-S., Lee, K.-H., Kim, C.-H., Kim, K.-Y., Kim, M.-G., 2007. Biotechnol. Bioprocess. Eng. 12, 80–85.
Ko, H.J., Park, T.H., 2005. Biosens. Bioelectron. 20, 1327–1332.
Ko, H.J., Park, T.H., 2006. Biol. Chem. 387, 59–68.
Krautwurst, D., Yau, K.-W., Reed, R.R., 1998. Cell 95, 917–926.
Lee, J.Y., Ko, H.J., Lee, S.H., Park, T.H., 2006. Enzyme Microb. Technol. 39, 375–380.
Lee, S.H., Jun, S.B., Ko, H.J., Kim, S.J., Park, T.H., 2009. Biosens. Bioelectron. 24, 2659–2664.
Liu, Q., Cai, H., Xu, Y., Li, Y., Li, R., Wang, P., 2006. Biosens. Bioelectron. 22, 318–322.
Malnic, B., Hirono, J., Sato, T., Buck, L.B., 1999. Cell 96, 713–723.
Marrakchi, M., Vidic, J., Jaffrezic-Renault, N., Martelet, C., Pajot-Augh, E., 2007. Eur. Biophys. J 35, 1015–1018.
Matarazzo, V., Clot-Faybesse, O., Marcet, B., Guiraudie-Capraz, G., Atanasova, B., Devauchelle, G., Cerutti, M., Etiévant, P., Ronin, C., 2005. Chem. Senses 30, 195–207.
Mazumdar, S.D., Hartmann, M., Kampfer, P., Keusgen, M., 2007. Biosens. Bioelectron. 22, 2040–2046.
Pfeiffer, J.R., Seagrave, J.C., Davis, B.H., Deanin, G.G., Oliver, J.M., 1985. J. Cell. Biol. 101, 2145–2155.
Rossi, C., Homand, J., Bauche, C., Hamdi, H., Ladant, D., Chopineau, J., 2003. Biochemistry 42, 15273–15283.
Singer, M.S., 2000. Chem. Senses 25, 155–165.
Stenlund, P., Babcock, G.J., Sodroski, J., Myszka, D.G., 2003. Anal. Biochem. 316, 243–250.
Sung, J.H., Ko, H.J., Park, T.H., 2006. Biosens. Bioelectron. 21, 1981–1986.
Vidic, J.M., Grosclaude, J., Persuy, M.-A., Aioun, J., Salesse, R., Pajot-Augy, E., 2006. Lab Chip 6, 1026–1032.
Vidic, J., Rla-Roca, M., Grosclaude, J., Persuy, M.-A., Monnerie, R., Caballero, D., Errachid, A., Hou, Y., Jaffrezic-Renault, N., Salesse, R., Pajot-Augy, E., Samitier, J., 2007. Anal. Chem. 79, 3280–3290.
Wetzel, C.H., Oles, M., Wellerdieck, C., Kuczkowiak, M., Gisselmann, G., Hatt, H., 1999. J. Neurosci. 19, 7426–7433.

Wu, C., Chen, P., Yu, H., Liu, Q., Zong, X., Cai, H., Wang, P., 2009. Biosens. Bioelectron. 24, 1498–1502.
Yanase, Y., Suzuki, H., Tsutsui, T., Hiragun, T., Kameyoshi, Y., Hide, M., 2007. Biosens. Bioelectron. 22, 1081–1086.
Zhang, J., Atay, T., Nurmikko, A.V., 2008. Nano Lett. 9, 519–524.
Zhao, H., Ivic, L., Otaki, J.M., Hashimoto, M., Mikoshiba, K., Firestein, S., 1998. Science 279, 237–242.